Akira Heya, Yoshihiro Nakata, Masahiko Sakai, Hiroshi Ishiguro, and Katsuhiro Hirata, "Force Estimation Method for a Magnetic Lead-Screw-Driven Linear Actuator," IEEE Transactions on Magnetics, vol.54, no.11, pp.1-5, Art no. 8207805, First published online: 13th, Aug., 2018; Issue published: Nov. 2018. DOI:10.1109/TMAG.2018.2845455

Force Estimation Method for a Magnetic Lead-Screw-Driven Linear Actuator

Akira Heya[1], Yoshihiro Nakata[2], Masahiko Sakai[1], Hiroshi Ishiguro[2], and Katsuhiro Hirata[1]
[1]Department of Adaptive Machine Systems, Osaka University, 2-1, Yamadaoka, Suita, Osaka 565-0871, Japan
[2]Department of Systems Innovation, Osaka University, 1-3, Machikaneyama, Toyonaka, Osaka 560-8531, Japan

Force-controllable actuators are essential for guaranteeing safety in human-robot interactions. Magnetic lead screws (MLSs) transfer force without requiring contact between parts. These devices can drive parts with high efficiency and no frictional contact, and they are force-limited when overloaded. We have developed a novel MLS that does not include spiral permanent magnets and a magnetic lead-screw-driven linear actuator (MLSDLA) that uses this device. This simple structure reduces the overall size of the device and improves productivity because of it is constructed by a commonly used machined screw as a screw. The actuator can drive back against an external force, and it moves flexibility based on the magnetic spring effect. In this paper, we propose a force estimation method for the MLSDLA that does not require separate sensors. The magnetic phase difference, as measured from the angular and linear displacement of the actuator, is used for this calculation. The estimated force is then compared, against measurements recorded with a load sensor in order to verify the effectiveness of the proposed method.

***Index Terms*—Magnetic lead screw, Linear actuator, Force estimation.**

I. Introduction

ROBOTS will soon work with humans and support them in collaborative, exoskeleton, and service roles [1][2]. In order to guarantee safety in these human-robot interactions, delicate force-controllable actuators are essential [3][4]. Furthermore, they must be lightweight, compact, and backdrivable.

We have been developing a magnetic lead-screw-driven linear actuator (MLSDLA) for use as a force-controllable actuator. This actuator consists of a magnetic lead screw (MLS) and a rotary motor.

An MLS is a kind of feed screw that allows noncontact power transmission. It is driven efficiently without frictional contact, and it is force-limited in case of overloading. The MLS is divided into two types; surface permanent magnet (SPM) type and interior permanent magnet (IPM) type. The SPMLSs use spiral shape radially magnetized permanent magnets [5]-[10] or small pieces of magnets placed in a spiral shape [11][12]. These SPMLSs have relatively high transmission force but it is difficult to manufacture them. In contrast, IPMLSs use a small number of simple shape magnets and teeth made of a soft magnetic material. These magnets are good availability and cost-effective. Paul proposed an IPMLS [13][14]. The rectangle permanent magnets are installed in a screw. Since robots need many actuators, better productivity (ease of manufacturing) of their actuators is essential. However, the conventional IPMLS needs the specially designed screw constructed by interior permanent magnets and iron core. When a long nut is needed, the nut length should be extended. The long nut is difficult to manufacture. Therefore, we proposed a moving-magnet type interior permanent magnetic lead screw (MM-IPMLS), it can be applied to a commonly used machined screw as a screw. The permanent magnets are installed in a nut. It is cost-effective, and it can easily extend the stroke by using the long screw in the same way as the feed screw or ball screw. The spiral structure is composed of a magnetic pole made of soft magnetic material and widely available arc-shaped permanent magnets. The force density of the MM-IPMLS is relatively smaller than SPMLSs, on the other hand it has high productivity and assemblability. The overall size of the MLS device can be made quite small thanks to this simple structure.

The MLSDLA designed with this structure exhibits backdrivability. Compliance can be realized because of the magnetic spring effect. The output force can be controllable with the rotation of the motor. Force sensors are generally required in order to control the force applied by a linear actuator. The inclusion of such sensors, however, increases the size and weight of the actuator. To solve this problem, several methods have been proposed for controlling the electric motor without a torque sensor [15][16]. We have been researching a control method for the MLSDLA that does not require force sensors. The static force applied by the MLSDLA is determined from the magnetic phase difference, which is indicated by the linear and angular displacement of the actuator. These values can be used to calculate the force supplied by the actuator at any moment.

This article details a force estimation method that exploits the magnetic phase difference in the MLSDLA. We fabricated a prototype of the MLSDLA and measured the force applied by the prototype with a sensor in order to compare the estimated force values with measurements.

II. Magnetic Lead-Screw-Driven Linear Actuator

This section describes the basic structure and operating principles of the proposed actuator and discusses the manufacture of the MLSDLA prototype.

This work was partially supported by JSPS KAKENHI (JP26700026 and JP17H04698). Manuscript received December 1, 2012; revised August 26, 2015. Corresponding author: A. Heya (email: akira.heya@ams.eng.osaka-u.ac.jp).

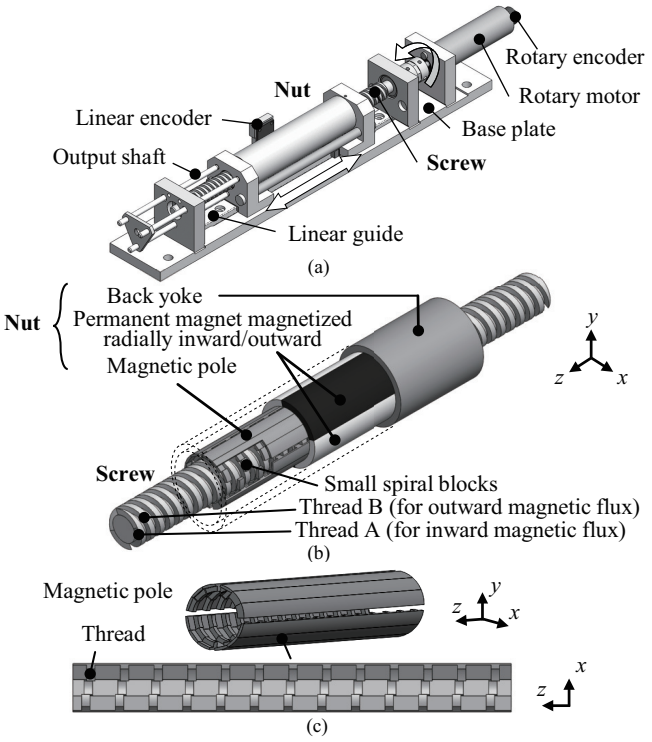

Fig. 1. Overview of the MLSDLA. (a) Basic structure of the MLSDLA. (b) Basic structure of the MM-IPMLS. The permanent magnets and back yoke are subsequently shown for showing internal structure. For visualizing the inner structure, one part of the magnetic pole is cut out. (c) Structure of the magnetic pole.

A. Basic Structure

The basic structure is shown in Fig. 1(a). The MLSDLA consists of an MM-IPMLS, a rotary motor, and linear and rotary encoders. The MM-IPMLS consists of a magnetic nut and magnetic screw. The screw does not require a spiral-shaped permanent magnet. The nut is fixed to a linear guide, so that it movers only along the axis of rotation. The screw is fixed to a base plate, and it is driven by a rotary motor.

The internal structure of the MM-IPMLS is shown in Fig. 1(b). The driving force from the screw to the nut is transmitted through magnetic coupling without any mechanical contact. The screw is a double-threaded screw made of soft magnetic material. It was fabricated using the same process for fabricating a normal slide screw. The magnetic pole, permanent magnets, and back yoke are arranged in the preceding order from inside to outside the device. The structure of the magnetic pole is shown in Fig. 1(c). The magnetic pole is constructed by the dividing into twelve parts, and has small blocks for composing a magnetic circuit. The arrangement relation between the magnetic pole and the screw is shown in Fig. 2. The small spiral blocks of the magnetic pole are faced on the thread of the screw.

The MM-IPMLS is composed of arc-shaped permanent magnets. Since the device does not require a spiral-shaped permanent magnet, it can be produced compactly and quickly.

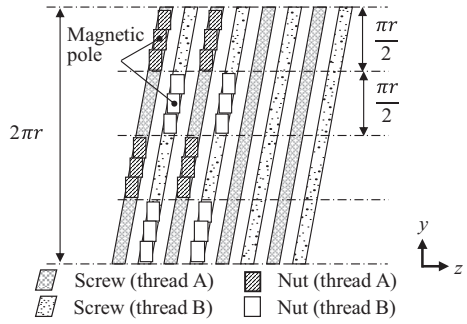

Fig. 2. Arrangement relation between the magnetic pole and the screw.

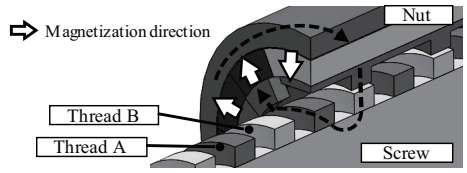

Fig. 3. Magnetic circuit of the MM-IPMLS.

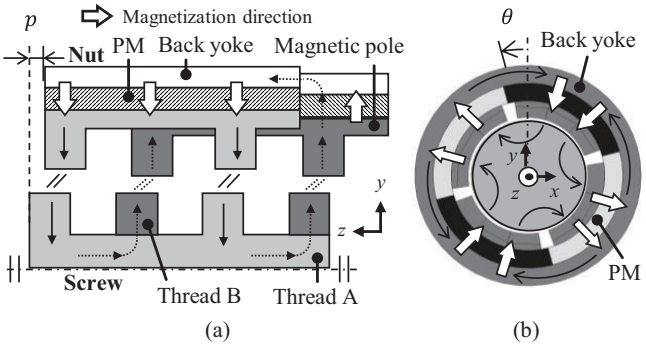

Fig. 4. Operating principle of the MM-IPMLS. (a) Rotational direction. (b) Translational direction.

B. Operating Principle

The magnetic circuit is shown in Fig. 3. The actuator is driven by the translation of the screw thread that is caused by the rotation of the screw by the rotary motor. An opposite force is generated when relative displacement between the nut and screw is caused by an external force (see Fig. 4). The nut returns to its equilibrium position because of this force. This restoring force provides the output force from the actuator. When the relative displacement between the nut and screw is over a quarter of the lead-screw length, the nut may step out.

C. Prototype

Static forces were analyzed in terms of electromagnetic fields using 3D finite element method (FEM) before manufacturing a prototype. The analysis conditions are listed in Table I. The parameters of the initial analysis model are shown in Fig. 5, and the dimensions are listed in Table II. A cross-sectional view of the magnetic flux density distribution is shown in Fig. 6. This figure shows that the proposed structure provides the appropriate magnetic coupling between the nut and the screw. The analysis results are shown in Fig. 9. According to the results, the maximum force that the actuator can produce is

TABLE I
ANALYSIS CONDITIONS

Number of elements	9,333,771
Number of nodes	2,837,937
CPU	Inter (R) Xeon (R) E5-1650 v3

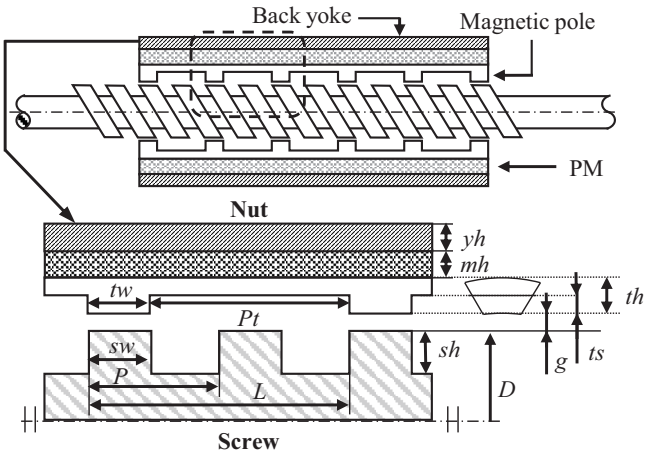

Fig. 5. Parameters of the Initial Analysis Model.

TABLE II
DIMENSIONS OF THE INITIAL ANALYSIS MODEL.

Part	Property	Variable	Value
Nut	Number of the magnetic pole pairs	n	4
	Radial thickness of the back yoke [mm]	yh	1.6
	Radial thickness of the PM [mm]	mh	1.6
	Angle of the divided PM [deg.]	$m\theta$	30
	Radial thickness of the magnetic pole [mm]	th	1.5
	Radial thickness of the teeth [mm]	ts	0.9
	Axial thickness of the teeth [mm]	tw	1.5
	Teeth pitch [mm]	Pt	6
Screw	Diameter	D	10
	Height of the screw thread	sh	1.5
	Axial thickness of the screw thread	sw	1.5
	Pitch	P	3
	Lead	L	6
	Air gap	g	0.3

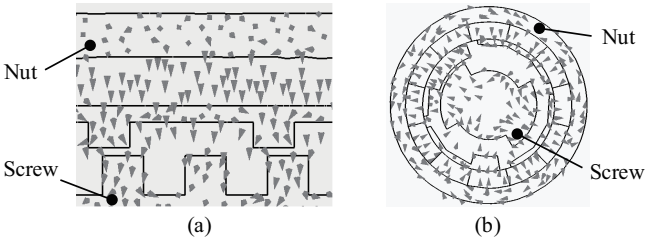

Fig. 6. Magnetic flux density distribution. (a) Cross-sectional view in the x-y plane. (b) Cross-sectional view in the y-z plane.

66.1 N. The results of the modified analysis model will be discussed in the section IV. C.

A prototype of the MLSDLA is shown in Fig. 7. The prototype is designed based on Table II. The MM-IPMLS is the smallest of the fabricated MLS [6][8][12]. The magnetic poles, back yoke, and screw are made of SUY. N48H permanent magnets were used for the nut, with a residual magnetic flux density and coercive force of 1.38 T and 1.10 $\times 10^6$ A/m, respectively. For fabricating the prototype, the permanent magnet are divided into three to circumferential direction, and are divided into two to axial direction.

The air gap is held by an oil-less bearing formed from resin. Moreover, a DC geared motor with a reduction ratio of 6.6 : 1 (DCX16L GB KL 12V, Maxon Motor AG) is used to drive the screw rotation. A linear optical encoder (AEDR-8500, 294LPI, Broadcom, Ltd.) detects the position of the nut. A rotary encoder (ENX10 EASY, Maxon Motor AG) measures the rotary angle of the motor to detect the rotary angle of the screw.

III. FORCE ESTIMATION FROM MAGNETIC PHASE DIFFERENCE

This section describes the method that we tested in order to estimate the actuator force on the basis of the magnetic phase difference between the nut and the screw.

A. Relationship between Static Force and Magnetic Phase Difference

The static force applied by the MM-IPMLS depends on the magnetic phase difference caused by the relative displacement between the nut and the screw. The magnetic phase differences in the rotational and translational direction are written as φ_θ and φ_p, respectively. The static force F_s is defined as a function of φ_θ or φ_p as follows:

$$F_s = \hat{F}_s(\varphi_\theta(\theta, p)) = \hat{F}_s(\varphi_p(\theta, p)) \tag{1}$$

where $\hat{F}_s$ is the estimated force, θ is the rotation angle of the screw, and p is the displacement of the nut relative to the screw. They are marked in Fig. 4. When the magnetic phase difference is zero, the rotational angle of the screw can be defined in terms of the nut displacement:

$$\theta_p = \frac{2\pi}{L} p \tag{2}$$

where L is the lead of the screw. The rotational magnetic phase difference φ_θ can be defined as a function of the nut position and screw rotation:

$$\varphi_\theta(\theta, p) = \theta - \theta_p \tag{3}$$

The static force is estimated from the rotational magnetic phase difference, which is calculated from measurements of the position of the nut and the rotational angle of the screw recorded using a linear optical encoder and a rotary encoder.

B. Consideration of the Dynamics of the Magnetic-Lead-Screw

The dynamics of the MM-IPMLS are given as by the following differential equation:

$$M_{ms}\ddot{p} + C_{ms}\dot{p} = F_s + F_f \tag{4}$$

where M_{ms} is mass of the nut, C_{ms} is the viscosity friction coefficient, and F_f is defined as follows:

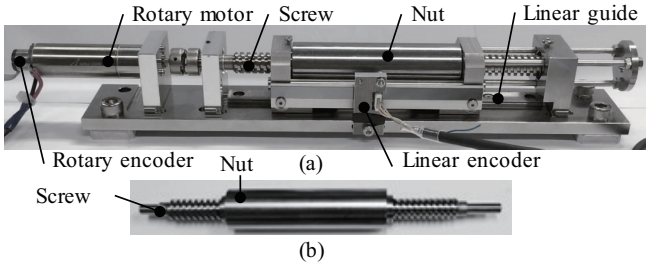

Fig. 7. Prototype of the MLSDLA. (a) Entire device. (b) Prototype of the MM-IPMLS.

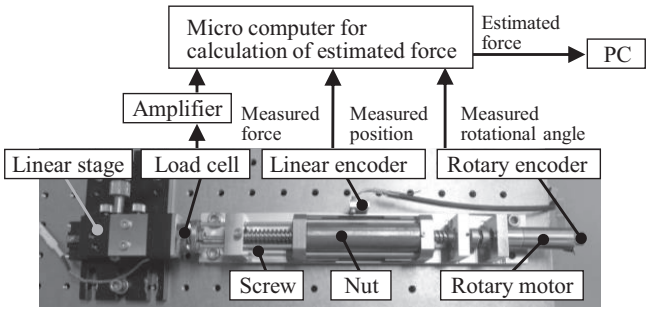

Fig. 8. Experiment environment.

$$F_f = F_c \mathrm{sign}(\dot{p}) \tag{5}$$

where F_c is the Coulomb friction. The estimated force is calculated as follows:

$$\hat{F}_{ms} = \hat{F}_s(\varphi_\theta(\theta, p)) + F_f \tag{6}$$

From Eq. (6), the estimated force is calculated from the nut position and rotation angle.

IV. Experimental Results

This section identifies the static characteristics of the prototype used for force estimation. The estimated and measured forces are compared. Then, the effectiveness of the proposed method and its limitations are discussed.

A. Experimental Setup

The experimental environment is shown in Fig. 8. The output force of the MLSDLA was measured with a load cell (LCM201-100N, Omega Engineering). This load cell is fixed to the linear stage and is connected to the nut of the MLSDLA via the output shafts. Measurements of the position and rotation angle are processed by a micro computer, and the estimated force is then calculated following the theoretical argument above. These data are recorded by a personal computer through serial communication. The measured rotation angle is also converted into the rotation angle of the screw.

B. Parameter Identification for Force Estimation

In this experiment, the output force of the MM-IPMLS was measured by constraining the rotational motion of the screw. The position of the nut was manually changed, and the nut is fixed by the linear stage. The restoring force is generated at each position, and is measured as the static force using the load cell. The measured static force characteristics are shown in Fig. 9. In this paper, the estimated force expressed as a polynomial approximation using the least-squares method is used for considering the end effect of the nut. The formulation is given as follows:

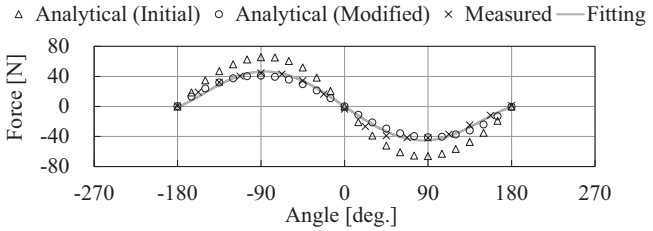

Fig. 9. Measured static force of the MM-IPMLS.

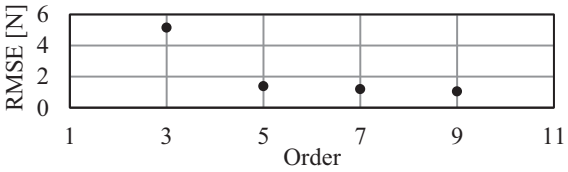

Fig. 10. Relationship between RMSE and the order of the regression equation.

$$\hat{F}_s = -0.378\varphi_\theta^5 - 0.209\varphi_\theta^4 + 8.51\varphi_\theta^3 + 2.59\varphi_\theta^2 - 47.6\varphi_\theta - 4.28 \tag{7}$$

A gap around the equilibrium point is corrected as an offset. The process of the curve fitting is a kind of calibration of the MLS. In the initial stage of the force estimation , this is required for every prototype.

The relationship between RMSE and the order of the equation is shown in Fig. 10. According to this data, 5 order is suitable because the differences among 5, 7, and 9 order are smaller than one between 3 and 5 order. The differences among 5, 7, and 9 are less than 0.5 N.

C. Comparison of Estimated and Measured Force

In this experiment, the output force was measured when external forces is applied.

1) Results

A comparison of the estimated and measured forces is shown in Fig. 11(a). The errors of the estimated and measured forces are shown in Fig. 11(b). The position of the nut and the rotation angle of the screw are shown in Fig. 11(c). The mean absolute error between the estimated and the measured forces is 2.3 N.

2) Discussion

According to Fig. 9, the percentage of the error to the analysis value at -90 deg. is 32.7%. The difference between measured and analysis values is not so small. This error is attributable to the manufacturing tolerances of the prototype. In the initial analytic model, the layer of binding material used for fixing the permanent magnets is also disregarded. The modified analysis model considered the binding material

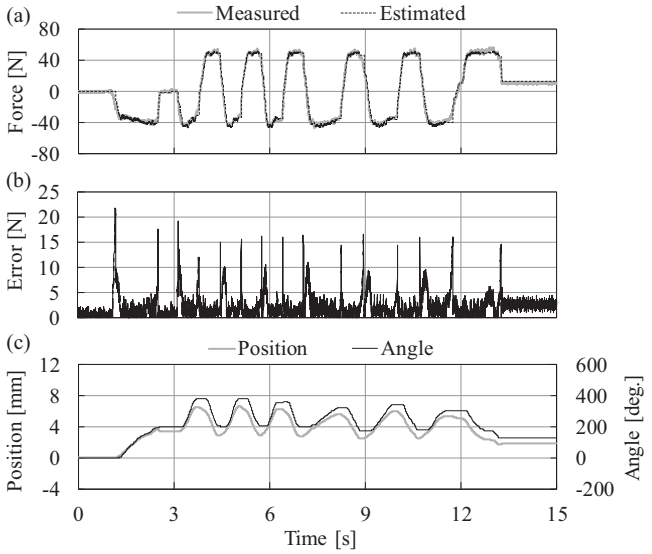

Fig. 11. Experimental results. (a) Comparison of the estimated and measured forces. (b) Errors of the estimated and measured forces. (c) Position of the nut and the rotation angle of the screw.

and the manufacturing tolerances, the width mh and angle $m\theta$ of the permanent magnet are shorten 0.14 mm and 1.5 deg., respectively. The air gap is widened 0.14 mm. As a result, it is confirmed that the measured and analytical values are in good agreement. This suggests that the force can be reduced caused by the binding material and manufacturing error.

In the prototype, the shear stress defined as a ratio of the stall force to the active area of the screw is 0.56 $\mathrm{MN/m^2}$. The force density defined as the force per active area is 0.14 $\mathrm{MN/m^2}$. This value is relatively smaller than ones of the MLSs developed by Holm et al. [6] and Ling et al [12]. However, these MLSs require a large number of permanent magnets to compose the spiral shape structure. On the other hand, the MM-IPMLS use a machined screw and a nut composed of arc shape magnets and teeth made of a soft magnetic material. They are easily mass-produces.

From Fig. 11, we conclude that the estimated and measured force values are in good agreement. A delay occurs at the start point and the peaks of force readings. The maximum estimated forces at this point exceed the maximum values of the measured static force. This phenomenon is explained by the Coulomb friction that occurs when moving the nut manually. In these experiment, F_c is 7.5 N. There are two main causes of the static friction. The friction is caused by oil-less bearing and linear guide. The air gap between the screw and the nut is maintained by the oil-less bearing. The nut is fixed to the linear guide to keep the position on the cross-section of the MLS. The attractive force between the screw and the nut increase the friction force.

The proposed method has several limitations though. Estimation errors are introduced in the least-squares approximation. In addition, this method cannot estimate forces that do not exceed the static frictional force when the positon of the nut remains constant. This problem can be solved by reducing of the static friction, which we leave for future work. Despite these limitations, we judge that force estimation without a force sensor is possible by measuring the phase difference between magnetically coupled elements generalized for use with MLSs that have different structures.

V. Conclusion

This article details a method for estimating the static force supplied by an MLSDLA without needing direct measurements from load cells. The structure and operating principles of the MLSDLA were described. A force estimation method that exploits magnetic phase differences was described. The estimated forces were compared with direct measurements using the MLSDLA prototype, and the value ware in good agreement with each other. In future work, the friction in the prototype in order to improve the estimation accuracy.

References

[1] H.-O. Lim and K. Tanie, "Human Safety Mechanisms of Human-Friendle Robots: Passive Viscoelastic Trunk and Passively Movable Base," *Inter. J. Robotics Reserch*, vol. 19, no. 4, Apr. 2000.

[2] D. Hyun, H. S. Yang, J. Park, and Y. Shim, "Variable Stiffness Mechanism for Human-Friendly Robots," *Mech. Mach. Theory*, vol. 45, no. 6, pp. 880-897, June 2010.

[3] F. Frioli, S. Wolf, M. Garabini, M. Catalano, E. Burdet, D. Caldwell, R. Carloni, W. Friedl, M. Grebenstein, M. Laffranchi, D. Lefeber, S. Stramigioli, N. Tsagarakis, M. V. Damme, B. Vanderborght, A. A.-Schaeffer, and A. Bicchi, "Variable stiffness actuators: The user's point of view," *Inter. J. Robotics Research*, vol. 34, no. 6, pp. 727-743, Mar. 2015.

[4] A. Jafari, G. Tsagarakis, and D. G. Caldwell, "AwAS-II: A New Actuator with Adjustable Stiffness based on the Novel Principle of Adaptable Pivot point and Variable Lever ratio," *IEEE Inter. Conf. Robotics Auto.*, pp. 4638-4643, May 2011

[5] J. Wang, K. Atallah, and W. Wang, "Analysis of a Magnetic Screw for High Force Density Linear Electromagnetic Actuators," *IEEE Trans. Magn.*, vol. 47, no. 10, pp. 4477-4480, Oct. 2011.

[6] R. K. Holm, N. I. Berg, M. Walkusch, P. O. Rasmussen, and R. H. Hansen, Design of a Magnetic Lead Screw for Wave Energy Conversion, *IEEE Trans. Ind. Appl.*, vol. 49, no. 6, pp. 2699-2708, Nov./Dec. 2013.

[7] N. I. Berg, R. K. Holm, and P. O. Rasmussen, Theoretical and Experimental Loss and Efciency Studies of a Masgnetic Lead Screw, *IEEE Trans. Ind. Appl.*, vol. 51, no. 2, pp. 1438-1445, Mar./Arp. 2015.

[8] S. Pakdelian and H. A. Toliyat, Magnetic Design Aspects of the Trans-Rotary Magnetic Gear, *IEEE Trans. Energy Convers.*, vol. 30, no. 1, pp. 1720-1725, Mar. 2015.

[9] S. Pakdelian, N. W. Frank, and H. A. Toliyat, Principle of the Trans-Rotary Magnetic Gear, *IEEE Trans. Mgn.*, vol. 49, no. 2, pp. 883-889, Feb. 2013.

[10] S. Pakdelian, Y. B. Deshpande, H. A. Toliyat, Design of an Electric Machine Integrated with Trans-Rotary Magnetic Gear, *IEEE Trans. Energy Convers.*, vol. 30, no. 3, pp. 1180-1191, Sep. 2015.

[11] Z. Ling, W. Zhao, J. Ji, and G. Liu, "Design of a New Magnetic Screw With Discretized PMs," *IEEE Trans. Appl. Supercond.*, vol. 26, no. 4, 0602805, June 2016.

[12] Z. Ling, J. Ji, J. Wang, and W. Zhao, Design Optimization and Test of a Radially Magnetized Magnetic Screw With Discretized PMs, *IEEE Trans. Ind. Electron.*, vol. 65, no. 9, pp. 7536-7547, Sept. 2018.

[13] R. J. A. Paul, Magnetic rotary-to-linear converter, *IEE J. Electric Power Appl.*, vol. 1, no. 4, pp. 115-116, Nov. 1978.

[14] R. J. A. Paul, Magnetic rotary-linear or linear-rotary convertor, *IEE J. Electric Power Appl.*, vol. 2, no. 4, pp. 135-138, Aug. 1979.

[15] A. Kato and K. Ohnishi, "Robust force sensorless control in motion control system," *IEEE Inter. Workshop Adv. Motion Control*, pp. 165-170, Mar. 2006.

[16] Y. Ohba, S. Katsuya, and K. Ohishi, "Sensor-less force control for machine tool using reaction torque observer," *IEEE Inter. Conf. Ind. Tech.*, pp. 860-865, Dec. 2006.